Two-Stage Stochastic Market Clearing of Energy and Reserve in the Presence of Coupled Fuel Cell-Based Hydrogen Storage System with Renewable Resources

Agabalaye-Rahvar, Masoud ; Mansour-Saatloo, Amin ; Mirazaei, Mohammad Amin ; Mohammadi-Ivatloo, Behnam ; Zare, Kazem; Anvari-Moghaddam, Amjad

Published in:
Power Systems

DOI (link to publication from Publisher):
10.1007/978-3-030-87653-1_11

Publication date:
2022

Document Version
Publisher's PDF, also known as Version of record

Chapter 11
Two-Stage Stochastic Market Clearing of Energy and Reserve in the Presence of Coupled Fuel Cell-Based Hydrogen Storage System with Renewable Resources

Masoud Agabalaye-Rahvar, Amin Mansour-Saatloo, Mohammad Amin Mirazaei, Behnam Mohammadi-Ivatloo, Kazem Zare, and Amjad Anvari-Moghaddam

11.1 Introduction

Environmental issues compelled managers to generate the required electricity with a minimal level of emission production. Related to the International Renewable Energy Agency (IRENA) reports, renewable's contribution would set nearly 86% of the whole power production by 2050 [1]. Among the renewable energy sources (RESs), wind energy sources (WESs) are the prominent technology that supplies more than one-third of the whole electricity demand by 2050 to decarbonize energy systems in the subsequent three decades. However, deploying WESs at a high penetration level leads to some challenges in power system scheduling. Variability and uncertainty nature are the crucial challenges of WESs to system operators, which require considerable flexibility [2, 3]. As Fig. 11.1 highlighted the importance of integrating WES by coupling hydrogen storage system (HSS) technology as much

M. Agabalaye-Rahvar (✉) · A. Mansour-Saatloo · M. A. Mirazaei · K. Zare
Faculty of Electrical and Computer Engineering, University of Tabriz, Tabriz, Iran
e-mail: m.agabalaye97@ms.tabrizu.ac.ir; amin_mnsr97@ms.tabrizu.ac.ir; kazem.zare@tabrizu.ac.ir

B. Mohammadi-Ivatloo
Department of Electrical and Electronics Engineering, Muğla Sıtkı Koçman University, Muğla, Turkey

Faculty of Electrical and Computer Engineering, University of Tabriz, Tabriz, Iran
e-mail: bmohammadi@tabrizu.ac.ir

A. Anvari-Moghaddam
Department of Energy Technology, Aalborg University, Aalborg, Denmark
e-mail: aam@energy.aau.dk

V. Vahidinasab, B. Mohammadi-Ivatloo (eds.), *Whole Energy Systems*, Power Systems, https://doi.org/10.1007/978-3-030-87653-1_11

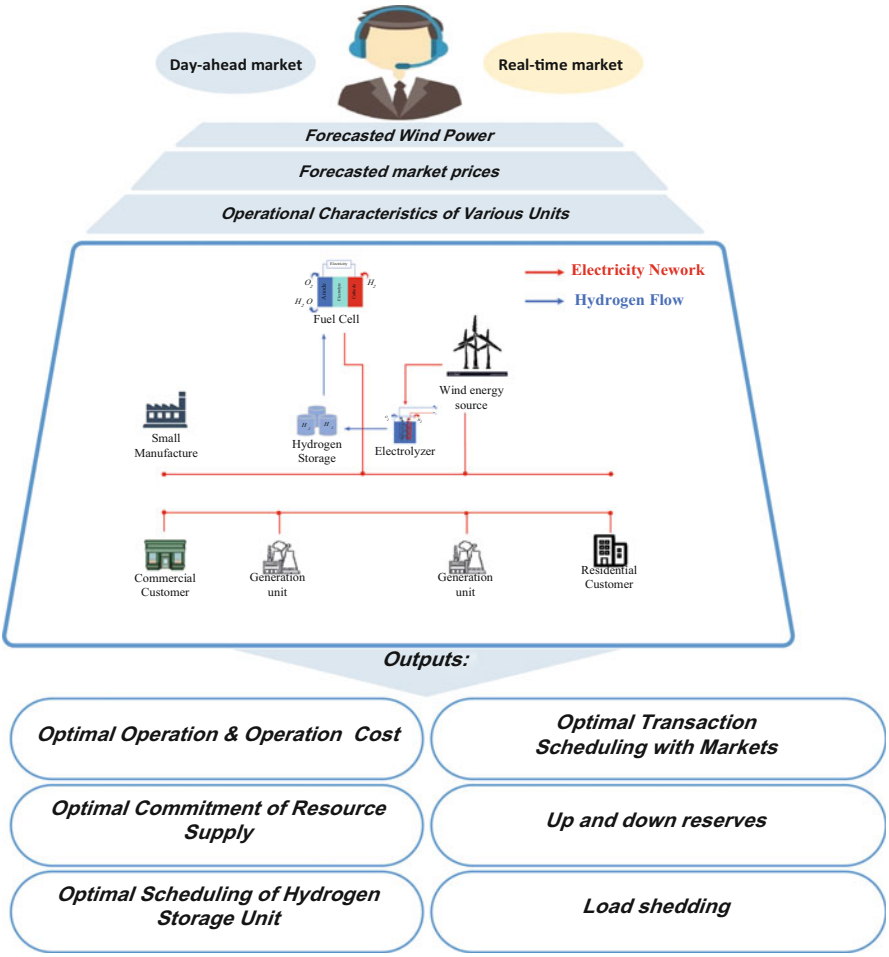

Fig. 11.1 The graphical representation for the whole integration of the hydrogen storage system into the electric power system

as possible into the electric power systems, achieving optimal scheduling in various energy markets is being indispensable.

The target of operational flexibility is supporting the mentioned challenges in a secure way with the least expenditures by deploying sufficient flexible resources. Generic solutions could be categorized into two main groups as novel market mechanism design and incorporation of flexible facilities. The first group emphasizes designing modern market mechanisms to provide flexibility procurement in system operation and management [4–6]. The second one is related to the integration of flexible facilities like environmental-friendly energy storages (EFESs), demand response programs (DRPs), and plug-in electric vehicles (PEVs) into the generation structure [7–10]. It is worth noting that the interest in applying these flexible

technologies worldwide is more considerable in recent decades. In [9], authors have proposed optimal energy management for a renewable-based microgrid (RMG) by considering PEVs as a flexible load to take part in DRPs to achieve maximum benefit in both energy and reserve markets. So, in [10], the integration of HSS technology as a clean energy source (CES) with WES by the interaction of DRP in the day-ahead energy market has been investigated. The novel HSS technology has become widely utilized due to its capability to support several critical energy challenges and also provides tremendous participation to RESs.

In recent decades, various researchers have studied the structure and implementation of HSS technology in power system optimization problems. In the power system integrated with HSS and WES introduced by [11], a risk-averse strategy accompanied by proposed downside risk constraint is analyzed. A modern power to hydrogen technology has been proposed in [12] for the optimal operation of multi-energy microgrids (MGs) in multi-energy markets. A robust scheduling methodology has been presented in [13] for a micro-energy hub (mEH), which is integrated with HSS and integrated demand response program (IDR) technologies. A bi-objective scheduling framework specified applying HSS in both economic and environmental aspects [14]. Also, in real operating projects, the interest of deploying HSS in a coordinated path has grown rapidly, similar to the research viewpoint. For instance, German transmission and gas net operators have represented an investment-ready scheme for a 100 MW electrolyzer and hydrogen pipeline, which could get online by 2023 [15]. In South Australia, a 30 MW electrolyzer incorporated with ammonia storage is organized in 2018 [16].

A lot of researches have centralized on the day-ahead security-constrained scheduling of electricity networks. All reviewed papers are separated into two principal groups. The first group is denoted the schedule of a day-ahead energy market problem. A bi-level programming approach is proposed in [17] to minimize consumer payment in the pool-based electricity market. In this approach, the generation's scheduling with a decreasing of the total consumer payment is stated in the upper level; however, the lower level included the determination of local marginal prices (LMPs) with a multi-period optimal power flow (MOPF). The hourly scheduling of centralized and decentralized energy storage systems (ESSs) for day-ahead electricity markets has been analyzed through [18]. Ref [19] has indicated the robust optimal strategy of the introduced energy system integrated with power-to-gas (P2G), gas-fired units, and WESs in energy markets. In [20], the authors have presented the optimal hourly network-constrained and dispatch of producing units in the day-ahead optimization problem by considering the charging/discharging schedule of EV batteries and user driving essentials. Two-stage network-constrained unit-commitment programming for the day-ahead energy market scheduling with DRPs is presented in [21]. In this paper, the first stage determines a network-constrained unit-commitment problem with DRP, whereas the second stage is relevant to the specification of the demand shifting/curtailment during the time horizon based on netload changes. Ref [20] has outlined an effective solution methodology called Benders' decomposition to solve the stochastic security-constrained AC unit-commitment problem. The proposed problem in [20]

is modeled as a two-stage stochastic programming problem, in which the first stage denotes the day-ahead energy market and the second stage demonstrates real-time operation. In [22], an optimal hourly day-ahead scheduling of combined heat and power (CHP) units and electrical/thermal energy storages (EESs/TESs), taking into account security constraints, have been addressed. Two-stage stochastic mixed-integer linear programming (SMILP) is deployed to solve the problem described in [22]. The coordinated multi-carrier energy system (MCES) with a robust/information gap decision theory (IGDT) methodology has been developed in [23] by considering the TESs facility. The second group of papers is relevant to the scheduling problem in day-ahead energy and reserve markets. Various time-based rate DRPs (TBRDRPs) are investigated in [24] to identify these effects on the day-ahead energy and reserve scheduling in the islanded residential MGs equipped with RESs and EVs. A novel predicted interval (PI) called adjustable intervals (AIs) is introduced in [25] to handle the wind power uncertainties and proposed an AI optimization method for energy and reserve market clearing accompanied by WES. Co-optimization of daily security-constrained energy and reserve markets under WES has been addressed in [26], which is formulated as a two-stage risk-averse optimization technique. To consideration of gas network besides the electricity network, a two-stage stochastic security-constrained model in energy and reserve markets with the integration of ESS and WES is represented by [27]. Most of the analyzed papers in the literature are not considered the integration of EFES and WES in the scheduling problem. Therefore, the importance of integrating HSS and WES in the energy and reserve market-clearing problem is much more indispensable and should be taken into account.

As the investigation and analysis of related works in the literature, a research gap is the coordination operation of integrated HSS and WES in the energy and reserve market-clearing process as the two-stage stochastic network-constrained energy and reserve scheduling. Thus, the present chapter concentrated on the proposed problem, along with consideration of fluctuations dependent on WES and electrical demand. Also, the effects of coupled HSS and WES on the load shedding and wind power curtailment are investigated to obtain minimal curtailments of the system. A suitable scenario decrement methodology is deployed to prevent the presentation of all produced scenarios and decrease the computational time. Finally, a comprehension illustrative of the proposed framework is demonstrated in Fig. 11.2. Thus, the principal contributions of the current chapter could be stated in the following:

1. A set of flexibility suppliers, including HSS technology and reserve services, is considered to increment the system's operational flexibility.
2. The integrated fuel cell-based HSS and WES are taken into account in the presented system to reduce the load shedding and wind power curtailment.
3. A two-stage stochastic network-constrained energy and reserve scheduling approach is proposed that the energy expenditure, scheduled and deployed reserves, load shedding, and wind power curtailment are considered.
4. The Monte Carlo simulation (MCS) algorithm is applied to satisfy the variability characteristic of electrical demand and WES to determine the system's hourly required reserve.

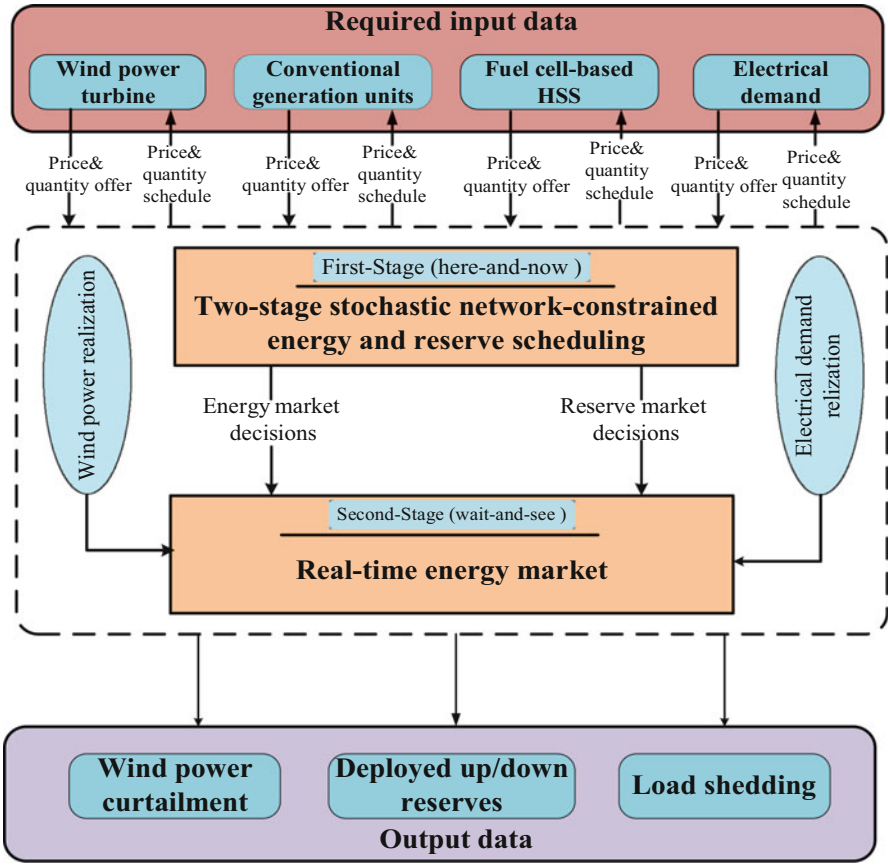

Fig. 11.2 The comprehension illustrative of the presented framework

The remainder of this chapter is categorized as the following: Sect. 11.2 presents the mechanism and impacts of HSS technology on system flexibility. The mathematical problem formulation is introduced in Sect. 11.3. Various case studies and simulation results are presented in Sect. 11.4. Eventually, in Sect. 11.5 is performed the conclusion such that Sect. 11.6 denotes the status quo, challenges, and outlooks.

11.2 Hydrogen Storage System Technology

11.2.1 Mechanism of HSS

Although more previous papers mainly focused on metal hydrides and carbon materials [28, 29], the other storing hydrogen substances like chemical storage and

physisorption are introduced in subsequent years [30, 31]. Hydrogen is produced through a chemical reaction by storing hydrogen materials such as ammonia, formic acid, carbohydrates, and liquid organic hydrogen carriers (LOHC) in the chemical-type storages. The other procedure to generate hydrogen is physisorption, which is a process that hydrogen molecules get adsorbed at the exterior of the substance. To preserve the molecular individuality of hydrogen could be achieved from porous materials as zeolites, metal-organic frameworks (MOFs), clathrates, and organotransition element associations.

The best standard energy conversion technologies are electrolysis and fuel cells (FCs). A clean procedure called electrolysis produces no utilizable greenhouse gases. Three fundamental types of water electrolyzer have existed as alkaline, polymer electrolyte membrane (PEM), and solid oxide [32]. However, FCs have a high electricity conversion efficiency from hydrogen energy, to nearly 50% [32]. It can be stated that FCs provide more advantages like covering the power system, decreasing air emissions, and enhancing the dependability of the system which are clarified in [33].

11.2.2 Facilitating the Accretion of RESs

Implementation of large-scale hydrogen energy could increment the request for RESs power generation. IRENA predicted a universal economic capability for 19 EJ of hydrogen from RESs power in the whole energy utilization up to 2050 [15]. Also, approximately 4–16 TW of solar and wind power capacity must be installed to procreate hydrogen and hydrogen-based products in 2050 [15]. Consequently, applying hydrogen energy at an appropriate scale of power system could provide remarkable outcomes for the power section and allocate further opportunities for RESs development.

11.2.3 Impacts of HSS on Increasing System Flexibility

Hydrogen electrolyzers could construct extra flexibility to a network-constrained power system. Modernized electrolyzers have the ability to ramp up and down in a few minutes or even seconds. PEM electrolyzers, in contrast to alkaline, are capable of responding faster, which is the one reason why they are prominent in the forthcoming studies. The problems related to power grid congestion and RESs electricity curtailment are solved by locating strategically electrolyzers. For instance, considering such strategic electrolyzers could be settled in the North sea area by developing offshore wind energy [15]. Thus, the countries have a selection to transfer RESs electricity through a copper wire or embedded in the form of hydrogen.

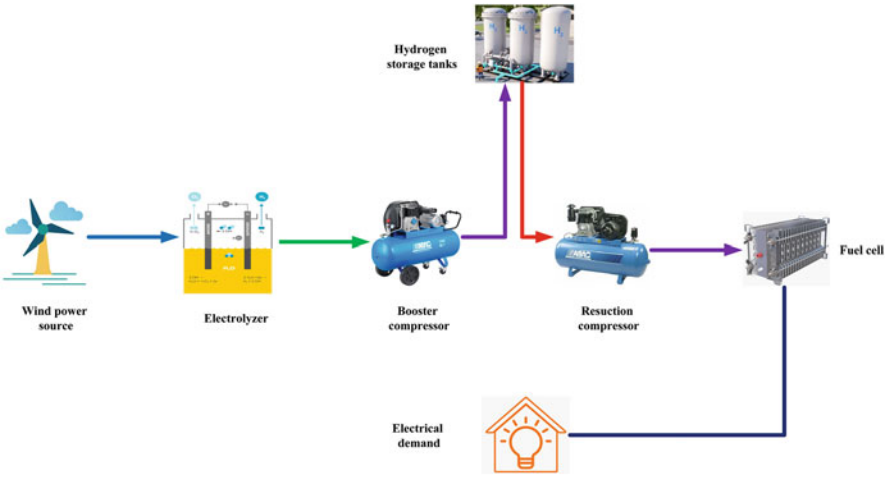

Fig. 11.3 The schematic composition of HSS technology

By these explanations, hydrogen energy could be generated from extra electricity production of other energy reservoirs, especially WES power production during low electricity demand or price via utilizing electrolyzers. The stored hydrogen in tanks could be reconverted to power through fuel cell-based HSS to satisfy peak demand. Therefore, a schematic structure of HSS technology has been illustrated in Fig. 11.3.

11.3 Problem Formulation

11.3.1 Modeling of Uncertain Nature

To tackle the fluctuations of WES and electrical demand, various methodologies have been studied and investigated by researchers [34, 35]. Wind power production has an undetermined characteristic due to variable wind speed data. The most practical approach to wind speed scenario generation is the Weibull probability density function (PDF) presented in Eq. (11.1). Finally, the output wind power production is calculated through Eq. (11.2). Besides, normal PDF is deployed to model the unpredictability of electrical demand, and this relation is defined as Eq. (11.3).

By these formulations, a vast quantity of scenarios is generated through the executing MCS algorithm. Thus, the fast backward forward selection approach is utilized to decrement the generated scenarios.

$$\mathrm{PDF}\left(v_t\right) = \left(\frac{\hat{k}}{\mathrm{sf}}\right)\left(\frac{v_t}{\mathrm{sf}}\right)^{\hat{k}-1}\exp\left(-\left(\frac{v_t}{\mathrm{sf}}\right)\right)^{\hat{k}} \tag{11.1}$$

$$P_{w,t}^{\mathrm{FWT}}\left(v_t\right) = \begin{cases} 0 & \text{if } v_t \le v^{\mathrm{CI}} \text{ or } v_t \ge v^{\mathrm{CO}} \\ \frac{v_t - v^{\mathrm{CI}}}{v^R - v^{\mathrm{CI}}} P_w^{\mathrm{WT},R} & \text{if } v^{\mathrm{CI}} \le v_t \le v^R \\ P_w^{\mathrm{WT},R} & \text{if } v^R \le v_t \le v^{\mathrm{CO}} \end{cases} \tag{11.2}$$

$$\mathrm{PDF}\left(\mathrm{PD}_{d,t}^{\mathrm{EL}}\right) = \frac{1}{\sqrt{2\pi\sigma_d^{\mathrm{EL}}}}\exp\left[-\frac{\left(\mathrm{PD}_{d,t}^{\mathrm{EL}} - \mu_d^{\mathrm{EL}}\right)^2}{2\left(\sigma_d^{\mathrm{EL}}\right)^2}\right] \tag{11.3}$$

where $\hat{k}$, sf are the shape and scale factors of the Weibull PDF; v^{CI},v^{CO}, and v^R are the cut-in, cut-out, and rated speed required for wind turbine w; $P_{w,t}^{\mathrm{FWT}}$, $P_w^{\mathrm{WT},R}$ are the forecasted and rated power of wind power turbine w; $\mathrm{PD}_{d,t}^{\mathrm{EL}}$ is the forecasted electrical demand d at time t; and μ_d^{EL} and σ_d^{EL} are the mean value and standard deviation of the electrical demand d.

11.3.2 Objective Function

The proposed energy and reserve scheduling problem includes the objective function, conventional generating units, and integrated fuel cell-based HSS with WES in both the first and second stages. The objective function in (11.4) minimizes the system's entire operation expenditure in the attendance of uncertainties by modeling the day-ahead and real-time market clearings. The power generation of conventional units contains energy costs, start-up costs, and scheduled up and down capacity reserve costs, which are indicated in the first line (11.4). The energy costs related to conventional units are considered the piecewise linear fuel costs function, located in the first term of the first line. The second line of (11.4) shows the costs relevant to discharging power and up and down capacity reserve via fuel cell-based HSS. The third line of (11.4) models the real-time market costs, which are denoted by the restorative conductions embedded in scenarios. Some principal actions that can be used to overcome the uncertainty of the electrical demand and WES are deployed up and down reserves by the traditional units and fuel cell-based HSS. The costs related to the load shedding and wind power curtailment in any scenario are presented in the third line's last two terms.

$$\begin{aligned}
&\text{Minimize} \\
&\sum_{t=1}^{\mathrm{NT}}\sum_{g=1}^{\mathrm{NCU}}\left[P_{g,t}^{\mathrm{CU}}C_{g,t}^{\mathrm{CUEg}}+\mathrm{SUC}_{g,t}^{\mathrm{CU}}+R_{g,t}^{\mathrm{CUSUP}}C_{g,t}^{\mathrm{CUSUP}}+R_{g,t}^{\mathrm{CUSDN}}C_{g,t}^{\mathrm{CUSDN}}\right] \\
&+\sum_{t=1}^{\mathrm{NT}}\sum_{h=1}^{\mathrm{NHS}}\left[P_{h,t}^{\mathrm{dis}}C_{h,t}^{\mathrm{HSEg}}+R_{h,t}^{\mathrm{HSSUP}}C_{h,t}^{\mathrm{HSSUP}}+R_{h,t}^{\mathrm{HSSDN}}C_{h,t}^{\mathrm{HSSDN}}\right] \\
&+\sum_{t=1}^{\mathrm{NT}}\sum_{k=1}^{\mathrm{NK}}p_k\left[\begin{array}{l}\sum_{g=1}^{\mathrm{NCU}}\left(r_{g,t,k}^{\mathrm{CUDUP}}C_{g,t}^{\mathrm{CUDUP}}-r_{g,t,k}^{\mathrm{CUDDN}}C_{g,t}^{\mathrm{CUDDN}}\right) \\ +\sum_{h=1}^{\mathrm{NHS}}\left(r_{h,t,k}^{\mathrm{HSDUP}}C_{h,t}^{\mathrm{HSDUP}}-r_{h,t,k}^{\mathrm{HSDDN}}C_{h,t}^{\mathrm{HSDDN}}\right) \\ +\sum_{w=1}^{\mathrm{NW}}P_{w,t,k}^{\mathrm{WPCurt}}C_{w,t}^{\mathrm{WPCurt}}+\sum_{d=1}^{\mathrm{ND}}\mathrm{Voll}_{d,t}^{\mathrm{EL}}\mathrm{LS}_{d,t,k}^{\mathrm{EL}}\end{array}\right]
\end{aligned} \tag{11.4}$$

where *t, g, h, k, w,* and *d* are indices of the time periods, conventional units, hydrogen storage systems, scenarios, wind power turbines, and electrical demands, respectively; $C_{g,t}^{\mathrm{CUEg}}$,$C_{g,t}^{\mathrm{CUSUP}}$, and $C_{g,t}^{\mathrm{CUSDN}}$ denote the offer costs of energy, scheduled upward reserve, and scheduled downward reserve for the conventional unit *g* at time *t*, respectively; $\mathrm{SUC}_{g,t}^{\mathrm{CU}}$ is the start-up cost for the conventional unit *g* at time *t*; $P_{g,t}^{\mathrm{CU}}$, $R_{g,t}^{\mathrm{CUSUP}}$, and $R_{g,t}^{\mathrm{CUSDN}}$ are the power production, scheduled upward reserve, and scheduled downward reserve for the conventional units *g* at time *t*, respectively; $P_{h,t}^{\mathrm{dis}}$, $R_{h,t}^{\mathrm{HSSUP}}$, and $R_{h,t}^{\mathrm{HSSDN}}$ are the discharge power, scheduled upward reserve, and scheduled downward reserve for the HSS unit *h* at time *t*, respectively; $C_{h,t}^{\mathrm{HSEg}}$, $C_{h,t}^{\mathrm{HSSUP}}$, and $C_{h,t}^{\mathrm{HSSDN}}$ are the offer costs of energy, scheduled upward reserve, and scheduled downward reserve for the HSS unit *h* at time *t*, respectively; $r_{g,t,k}^{\mathrm{CUDUP}}$ and $r_{g,t,k}^{\mathrm{CUDDN}}$ represent the deployed upward and downward reserves for the conventional unit *g* at time *t* in scenario *k*, while $r_{h,t,k}^{\mathrm{HSDUP}}$ and $r_{h,t,k}^{\mathrm{HSDDN}}$ represent for the HSS unit *h* at time *t* in scenario *k*; $C_{g,t}^{\mathrm{CUDUP}}$ and $C_{g,t}^{\mathrm{CUDDN}}$ are the offer costs of deployed upward and downward reserves for the conventional unit *g* at time *t*, while $C_{h,t}^{\mathrm{HSDUP}}$ and $C_{h,t}^{\mathrm{HSDDN}}$ are for the HSS unit *h* at time *t*; $C_{w,t}^{\mathrm{WPCurt}}$ and $\mathrm{Voll}_{d,t}^{\mathrm{EL}}$ are the costs of the wind power curtailment in wind turbine *w* at time *t* and load shedding of electrical demand *d* at time *t*; and $P_{w,t,k}^{\mathrm{WPCurt}}$ and $\mathrm{LS}_{d,t,k}^{\mathrm{EL}}$ are the amount of wind power curtailment *w* at time *t* in scenario *k* and load shedding of electrical demand *d* at time *t* in scenario *k*.

11.3.3 First Stage

In the first stage of the proposed problem, the electric system constraints include conventional units, fuel cell-based HSS, WES, and transmission network constraints that are represented in (11.5, 11.6, 11.7, 11.8, 11.9, 11.10, 11.11, 11.12, 11.13, 11.14, 11.15, 11.16, 11.17, 11.18, 11.19, 11.20, 11.21, 11.22, 11.23, 11.24, 11.25, 11.26, and 11.27). The offered up and down reserve capacity through the conventional units in the day-ahead reserve market is influenced by the generation units' maximum reserve capacity, expressed by (11.5 and 11.6). The best feature of adding up and down reserve to the dispatched power units is to offer maximum and minimum power capacity into the energy and reserve markets, as stated in (11.7 and 11.8). The conventional units' up and down ramp rate constraints between two sequential hours are introduced in (11.9, 11.10, 11.11, and 11.12). In addition, these units must be turned on or off for specific hours before switching the status to off or on, respectively, which are presented by (11.13 and 11.14).

$$0 \le R_{g,t}^{\mathrm{CUSUP}} \le R_g^{\mathrm{Max\ UP}} \tag{11.5}$$

$$0 \le R_{g,t}^{\mathrm{CUSDN}} \le R_g^{\mathrm{Max\ DN}} \tag{11.6}$$

$$P_{g,t}^{\mathrm{CU}} + R_{g,t}^{\mathrm{CUSUP}} \le P_g^{\mathrm{Max}} I_{g,t} \tag{11.7}$$

$$P_{g,t}^{\mathrm{CU}} - R_{g,t}^{\mathrm{CUSDN}} \ge P_g^{\mathrm{Min}} I_{g,t} \tag{11.8}$$

$$P_{g,t}^{\mathrm{CU}} - P_{g,t-1}^{\mathrm{CU}} \le \left(1 - X_{g,t}\right) R_g^{\mathrm{RU}} + X_{g,t} P_g^{\mathrm{Min}} \tag{11.9}$$

$$P_{g,t-1}^{\mathrm{CU}} - P_{g,t}^{\mathrm{CU}} \le \left(1 - Y_{g,t}\right) R_g^{\mathrm{RD}} + Y_{g,t} P_g^{\mathrm{Min}} \tag{11.10}$$

$$X_{g,t} - Y_{g,t} \le I_{g,t} - I_{g,t-1} \tag{11.11}$$

$$X_{g,t} + Y_{g,t} \le 1 \tag{11.12}$$

$$\left(Z_{g,t-1}^{\mathrm{UPT}} - T_g^{\mathrm{UPT}}\right)\left(I_{g,t-1} - I_{g,t}\right) \ge 0 \tag{11.13}$$

$$\left(Z_{g,t-1}^{\mathrm{DNT}} - T_g^{\mathrm{DNT}}\right)\left(I_{g,t} - I_{g,t-1}\right) \ge 0 \tag{11.14}$$

where $R_g^{\text{Max UP}}$, $R_g^{\text{Max DN}}$ are the maximum upward and downward reserve capacities of the conventional unit g; P_g^{Max}, P_g^{Min} are the maximum and minimum power capacity of the conventional unit g; R_g^{RU}, R_g^{RD} are the ramp-up and ramp-down rates of the conventional unit g; $X_{g,t}$, $Y_{g,t}$ are the start-up and shutdown binary decision variables of the conventional unit g at time t, while $Z_{g,t-1}^{\text{UPT}}$, $Z_{g,t-1}^{\text{DNT}}$ are the up-time and down-time of conventional unit g before at time t; T_g^{UPT}, T_g^{DNT} represent the minimum up-time and down-time of the conventional unit g; and $I_{g,t}$ is the binary decision variable for the commitment status of the conventional unit g at time t.

HSS, like other energy storages, has two operating modes. The hourly scheduled up and down reserves offered by the fuel cell-based HSS in the day-ahead markets are indicated by (11.15 and 11.16). These reserves depend on the maximum reserve capability of these units. Constraints (11.17 and 11.18) are limited to the discharge and charge power of the HSS facility to the corresponding maximum values to take part in both energy and reserve markets. Constraint (11.19) is applied to avoid operating both modes of HSS simultaneously. The amount of hydrogen cumulative in the hydrogen tanks in every hour is calculated through (11.20), and the minimum and maximum capacity of HSS tanks restricted the hydrogen stored as expressed in (11.21). Besides, (11.22) determines the definite initial value of stored hydrogen in containers, and also, the initial and final stored hydrogen must be equal in each day, which is denoted by Eq. (11.23). Constraint (11.24) is deployed to consider the WES coupled with HSS technology.

$$0 \le R_{h,t}^{\text{HSSUP}} \le R_h^{\text{Max UP}} \tag{11.15}$$

$$0 \le R_{h,t}^{\text{HSSDN}} \le R_h^{\text{Max DN}} \tag{11.16}$$

$$0 \le P_{h,t}^{\text{dis}} + R_{h,t}^{\text{HSSUP}} \le P_h^{\text{Max,dis}} u_{h,t}^{\text{dis}} \tag{11.17}$$

$$0 \le P_{h,t}^{\text{ch}} + R_{h,t}^{\text{HSSDN}} \le P_h^{\text{Max,ch}} u_{h,t}^{\text{ch}} \tag{11.18}$$

$$u_{h,t}^{\text{dis}} + u_{h,t}^{\text{ch}} \le 1 \tag{11.19}$$

$$E_{h,t} = E_{h,t-1} + P_{h,t}^{\text{ch}} \eta_h^{\text{ch}} - \frac{P_{h,t}^{\text{dis}}}{\eta_h^{\text{dis}}} \tag{11.20}$$

$$E_h^{\text{Min}} \le E_{h,t} \le E_h^{\text{Max}} \tag{11.21}$$

$$E_{h,0} = E_h^{\mathrm{Ini}} \tag{11.22}$$

$$E_{h,0} = E_{h,\mathrm{NT}} \tag{11.23}$$

$$0 \le P_{w,t}^{\mathrm{WT}} \le P_{w,t}^{\mathrm{FWT}} \tag{11.24}$$

where $R_h^{\mathrm{Max\ UP}}$,$R_h^{\mathrm{Max\ DN}}$ are the maximum upward and downward reserve capacities of the HSS unit h; $P_h^{\mathrm{Max,dis}}$, $P_h^{\mathrm{Max,ch}}$ are the maximum discharging and charging power capacities of the HSS unit h; η_h^{dis}, η_h^{ch} are the efficiencies of the discharging and charging power of the HSS unit h; $u_{h,t}^{\mathrm{dis}}$, $u_{h,t}^{\mathrm{ch}}$ are discharging and charging binary decision variables of the HSS unit h at time t; E_h^{Max}, E_h^{Min}, and E_h^{Ini} are the maximum, minimum, and initial energy of the HSS unit h, respectively; $E_{h,0}$, $E_{h,\mathrm{NT}}$ are the existing energy in the beginning and ending time of the HSS unit h; $P_{w,t}^{\mathrm{WT}}$ is the dispatched power of wind turbine w at time t; and $P_{h,t}^{\mathrm{ch}}$ is the charge power for the HSS unit h at time t.

In the following equations, the system constraints are taken into account. For each bus of the system, the power balance is provided with Eq. (11.25), DC power flow in each line is determined via Eq. (11.26), and also, constraint (11.27) limited the line power transmission to the line capacity limitations.

$$\sum_{g=1}^{\mathrm{NCU}_b} P_{g,t}^{\mathrm{CU}} + \sum_{w=1}^{\mathrm{NW}_b} P_{w,t}^{\mathrm{WT}} + \sum_{h=1}^{\mathrm{NHS}_b} P_{h,t}^{\mathrm{dis}} - \sum_{h=1}^{\mathrm{NHS}_b} P_{h,t}^{\mathrm{ch}} - \sum_{d=1}^{\mathrm{ND}_b} \mathrm{PD}_{d,t}^{\mathrm{EL}} = \sum_{l=1}^{\mathrm{NL}_b} \mathrm{PT}_{l,t} \tag{11.25}$$

$$\mathrm{PT}_{l,t} = \frac{\delta_{b,t} - \delta_{\tilde{b},t}}{X_l} \tag{11.26}$$

$$-\mathrm{PT}_l^{\mathrm{Max}} \le \mathrm{PT}_{l,t} \le \mathrm{PT}_l^{\mathrm{Max}} \tag{11.27}$$

where $PT_{l,t}$, $\delta_{b,t}$ are the power transmitted of the line l at time t and the voltage angle of the bus b at time t and $\mathrm{PT}_l^{\mathrm{Max}}$,$X_l$ are the maximum capacity and the reactance of transmission line l.

11.3.4 Second Stage

In this stage of the proposed problem, the uncertainty and forecasted errors related to the electrical demand and WES are considered by deploying the decreased scenarios. Meanwhile, the scheduled up and down hourly reserves in the first stage

are changing to meet the variations of electrical demand and WES fluctuations. In constraints (11.28, 11.29, 11.30, and 11.31), the interconnection relationships among the deployed and scheduled hourly reserves from the first and second stages are indicated. In each considered scenario, the deployed up and down reserves cannot transgress the scheduled reserves from the conventional units and also from fuel cell-based HSS technology. Consequently, Eqs. (11.32, 11.33, and 11.34) are expressing the power produced by conventional units and HSS facility in a per scenario, which is obtained through the summation of scheduled power from the first stage and deployed reserves from the second stage. The up and down ramp rate limitations of conventional units between sequential hours for each scenario are defined as (11.35 and 11.36). Constraint (11.37) is described as considering the hydrogen stored in HSS in each hour and scenario in which the amount of hydrogen stored is restricted by (11.38). In addition, the initial and final values should be equal with each other in each scenario and per day, as denoted in (11.39). When the deployed reserves in each scenario could not maintain the power balance, the system's indispensable load shedding must be applied. So, the wind power curtailment and load shedding in each scenario are limited by (11.40 and 11.41). Finally, the real-time power balance constraint is shown in (11.42), and each line power transferred in any scenario is specified as (11.43 and 11.44).

$$0 \le r_{g,t,k}^{\mathrm{CUDUP}} \le R_{g,t}^{\mathrm{CUSUP}} \tag{11.28}$$

$$0 \le r_{g,t,k}^{\mathrm{CUDDN}} \le R_{g,t}^{\mathrm{CUSDN}} \tag{11.29}$$

$$0 \le r_{h,t,k}^{\mathrm{HSDUP}} \le R_{h,t}^{\mathrm{HSSUP}} \tag{11.30}$$

$$0 \le r_{h,t,k}^{\mathrm{HSDDN}} \le R_{h,t}^{\mathrm{HSSDN}} \tag{11.31}$$

$$P_{g,t,k}^{\mathrm{CU}} = P_{g,t}^{\mathrm{CU}} + r_{g,t,k}^{\mathrm{CUDUP}} - r_{g,t,k}^{\mathrm{CUDDN}} \tag{11.32}$$

$$P_{h,t,k}^{\mathrm{dis}} = P_{h,t}^{\mathrm{dis}} + r_{h,t,k}^{\mathrm{HSDUP}} \tag{11.33}$$

$$P_{h,t,k}^{\mathrm{ch}} = P_{h,t}^{\mathrm{ch}} + r_{h,t,k}^{\mathrm{HSDDN}} \tag{11.34}$$

$$P_{g,t,k}^{\mathrm{CU}} - P_{g,t-1,k}^{\mathrm{CU}} \le \left(1 - X_{g,t}\right) R_{g}^{\mathrm{RU}} + X_{g,t} P_{g}^{\mathrm{Min}} \tag{11.35}$$

$$P_{g,t-1,k}^{\mathrm{CU}} - P_{g,t,k}^{\mathrm{CU}} \leq \left(1 - Y_{g,t}\right) R_g^{\mathrm{RD}} + Y_{g,t} P_g^{\mathrm{Min}} \tag{11.36}$$

$$E_{h,t,k} = E_{h,t-1,k} + P_{h,t,k}^{\mathrm{ch}} \eta_h^{\mathrm{ch}} - \frac{P_{h,t,k}^{\mathrm{dis}}}{\eta_h^{\mathrm{dis}}} \tag{11.37}$$

$$E_h^{\mathrm{Min}} \leq E_{h,t,k} \leq E_h^{\mathrm{Max}} \tag{11.38}$$

$$E_{h,0,k} = E_{h,\mathrm{NT},k} = E_{h,0} \tag{11.39}$$

$$0 \leq P_{w,t,k}^{\mathrm{WPCurt}} \leq P_{w,t,k}^{\mathrm{WT}} \tag{11.40}$$

$$0 \leq LS_{d,t,k}^{\mathrm{EL}} \leq \mathrm{PD}_{d,t,k}^{\mathrm{EL}} \tag{11.41}$$

$$\begin{aligned} &\sum_{g=1}^{\mathrm{NCU}_b} P_{g,t,k}^{\mathrm{CU}} + \sum_{w=1}^{\mathrm{NW}_b} \left(P_{w,t,k}^{\mathrm{WT}} - P_{w,t,k}^{\mathrm{WPCurt}}\right) + \sum_{h=1}^{\mathrm{NHS_b}} P_{h,t,k}^{\mathrm{dis}} - \sum_{h=1}^{\mathrm{NHS}_b} P_{h,t,k}^{\mathrm{ch}} \\ &- \sum_{d=1}^{\mathrm{ND}_b} \left(\mathrm{PD}_{d,t,k}^{\mathrm{EL}} - \mathrm{LS}_{d,t,k}^{\mathrm{EL}}\right) = \sum_{l=1}^{\mathrm{NL}_b} \mathrm{PT}_{l,t,k} \end{aligned} \tag{11.42}$$

$$\mathrm{PT}_{l,t,k} = \frac{\delta_{b,t,k} - \delta_{\tilde{b},t,k}}{X_l} \tag{11.43}$$

$$-\mathrm{PT}_l^{\mathrm{Max}} \leq \mathrm{PT}_{l,t,k} \leq \mathrm{PT}_l^{\mathrm{Max}} \tag{11.44}$$

where $P_{g,t,k}^{\mathrm{CU}}$ is the power production of the conventional unit g at time t in scenario k; $P_{h,t,k}^{\mathrm{dis}}$,$P_{h,t,k}^{\mathrm{ch}}$ are the discharging and charging power of the HSS unit h at time t in scenario k; $E_{h,\,t,\,k}$ is the stored hydrogen energy of the HSS unit h at time t in scenario k; $P_{w,t,k}^{\mathrm{WT}}$ is the dispatched wind power turbine w at time t in scenario k; $\mathrm{PD}_{d,t,k}^{\mathrm{EL}}$ is the electrical power demand d at time t in scenario k; and $\mathrm{PT}_{l,\,t,\,k}$, $\delta_{b,\,t,\,k}$ are the power transmitted of the line l at time t in scenario k and the voltage angle of the bus b at time t in scenario k.

11.4 Case Studies

11.4.1 Test System and Data

The modified six-bus test system, as illustrated in Fig. 11.4, is composed of three gas-fueled generation units at buses 1, 2, and 6 and three electrical demands at buses 3, 4, and 5. Buses are linked to each other via seven transportation lines. All techno-economic data of the system is taken from [36]. The system is modified by using the hydrogen storage system and wind turbine with a power capacity of 30MW on bus 5. HSS technical data are reported in Table 11.1. Also, wind power curtailment and load shedding costs are 50$/MWh and 400$/MWh, respectively. Expenditures of up and down scheduled reserves for G1, G2, and G3 units are equal to 8, 10, and 11 $/MW, respectively. The start-up expenditure of these conventional units is equal to 500$/MW. Besides, the providing energy cost by the HSS unit is equal to 2$/MWh, and the scheduled reserve capacity costs by this unit are equivalent to 50% of the energy proposed cost. To deal with system uncertainties, 1000 scenarios were generated for both wind power and electrical demand based on the MCS approach using Weibull and normal PDFs, respectively. Thus, the number of scenarios was reduced to 10, utilizing the SCENRED tool in General Algebraic Modeling System (GAMS) software. The forecasted electrical demand and wind power production profiles are indicated in Fig. 11.5. According to the final reduced scenarios introduced in Table 11.2, the realization of the forecasted parameters can be accomplished.

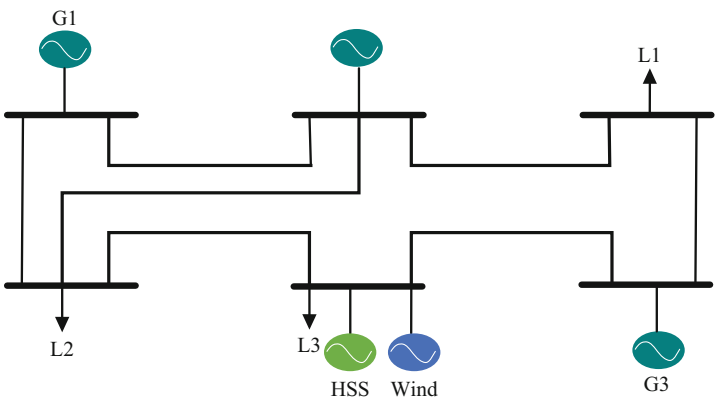

Fig. 11.4 The proposed six-bus electrical test system with WES and HSS units

Table 11.1 HSS technical data

Parameter	E_h^{Min} (MW)	E_h^{Max} (MW)	E_h^{Ini} (MW)	$P_h^{\text{Max,dis}}$ (MW)	$P_h^{\text{Max,ch}}$ (MW)	η_h^{dis} (%)	η_h^{ch} (%)
Value	40	180	70	30	30	80	80

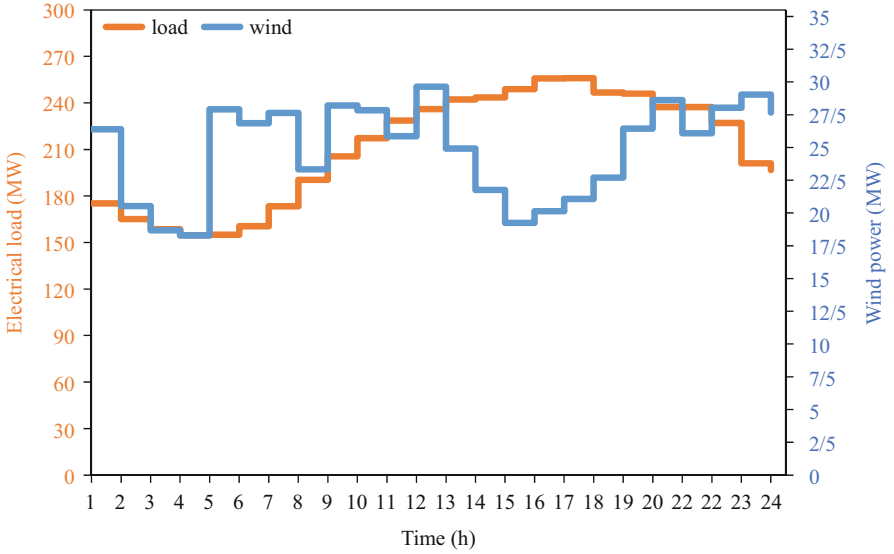

Fig. 11.5 The forecasted electrical load and wind power production profiles

Table 11.2 The probability and variations of each selected scenario

Scenario no.	Probability	Variations
1	0.26	−0.0176
2	0.12	+0.0442
3	0.08	+0.0507
4	0.07	+0.0087
5	0.14	−0.01198
6	0.09	−0.0305
7	0.02	+0.0532
8	0.07	−0.0021
9	0.07	−0.0182
10	0.08	+0.0532

11.4.2 Simulation and Analysis of Results

In this chapter, according to the above described two subsections, an electric six-bus test system along with a WES and fuel cell-based HSS is taken into account for investigating the application of the introduced model. The effects of the proposed coupled fuel cell-based HSS technology with WES on the costs of energy, reserve, wind power curtailment, and load shedding have been analyzed. To model the system uncertainties, i.e., the error of forecasting electrical demand and WES production, the MCS algorithm has been applied to generate the acceptable scenario sets. The presented problem formulation is modeled as a mixed-integer linear programming (MILP) model to implement in GAMS software, which is

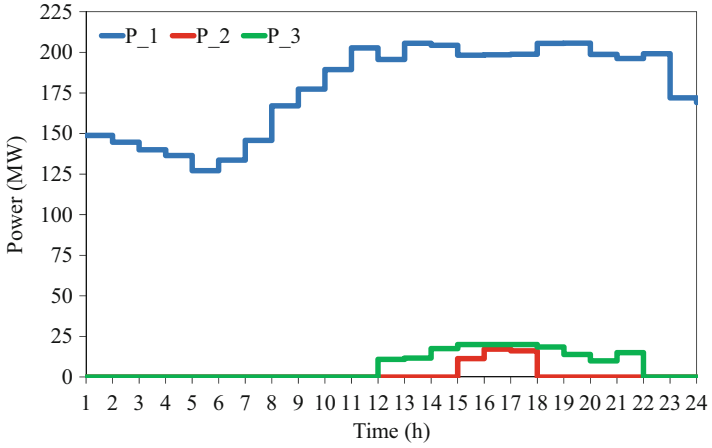

Fig. 11.6 Hourly power generation in Case 1

solved using CPLEX 12.9.0 solver. CPLEX solver especially utilizes branch and cut methodology and assigns the optimal solutions [37].

To study and analyze the obtained results of the presented problem, two case studies are taken into account as the following:

Case 1: Synchronous clearing of energy and reserve markets without consideration of fuel cell-based HSS technology

Case 2: Synchronous clearing of energy and reserve markets with consideration of fuel cell-based HSS technology

Case 1 In this case, all transmission line capacity restrictions are applied except the effects of fuel cell-based HSS on energy and reserve markets. As depicted in Fig. 11.6, the low-cost unit G1 is committed during the whole scheduling time horizon, whereas the high-cost unit G2 is committed only in peak hours, i.e., hours 15–17. The medium-cost unit G3 dispatches between hours 11 and 22 to meet the rest of the electrical demand in these hours. Table 11.3 reports all local marginal prices (LMPs) each hour to specify LMPs in the proposed modified test system with the mentioned techno-economic data. The provided LMPs are obtained via the joint energy and reserve market-clearing methodology. As reported in Table 11.3, the LMPs of all buses except bus 1 during hours 11, 14, and 18, which these rows highlighted in black, reached the maximum values, i.e., about 107 $/MWh. In reality, due to the transmission line restrictions, congestion of lines, and the obtained optimal power generations of conventional units, nearly all of the load shedding has occurred in hours 11, 14, and 18. As it can be seen in these three hours, the LMP of bus 4 has achieved the highest quantity of price compared to the rest buses. In the last column of Table 11.3, the average LMPs (Avg.LMPs) are increased by the growth of demand except in hours 11, 14, and 18.

Table 11.3 LMPs of all six buses in Case 1

Time (h)	Bus_1	Bus_2	Bus_3	Bus_4	Bus_5	Bus_6	Avg.LMPs
LMP($/MWh)							
1	13.51	13.51	13.51	13.51	13.51	13.51	13.51
2	13.51	13.51	13.51	13.51	13.51	13.51	13.51
3	13.51	13.51	13.51	13.51	13.51	13.51	13.51
4	13.51	13.51	13.51	13.51	13.51	13.51	13.51
5	13.51	13.51	13.51	13.51	13.51	13.51	13.51
6	13.51	13.51	13.51	13.51	13.51	13.51	13.51
7	13.51	13.51	13.51	13.51	13.51	13.51	13.51
8	13.51	13.51	13.51	13.51	13.51	13.51	13.51
9	13.51	13.51	13.51	13.51	13.51	13.51	13.51
10	13.51	13.51	13.51	13.51	13.51	13.51	13.51
11	**13.51**	**95.36**	**126.3**	**140.7**	**134.9**	**132.1**	**107.2**
12	13.51	15.09	15.61	15.90	15.88	15.80	15.32
13	13.51	26.53	31.46	33.75	32.83	32.83	28.41
14	**13.51**	**95.86**	**127.0**	**141.5**	**135.7**	**132.8**	**107.7**
15	13.51	23.92	27.86	29.70	28.96	28.60	25.43
16	13.51	32.63	39.86	43.23	41.88	41.22	35.39
17	13.51	32.63	39.86	43.23	41.88	41.22	35.39
18	**13.51**	**95.86**	**127.0**	**141.5**	**135.7**	**132.8**	**107.7**
19	13.51	44.23	55.86	61.28	59.10	58.04	48.67
20	13.51	15.09	15.69	15.97	15.85	15.80	15.32
21	13.51	15.69	16.52	16.91	16.75	16.68	16.02
22	13.51	25.76	30.40	32.56	31.69	31.27	27.53
23	13.51	13.51	13.51	13.51	13.51	13.51	13.51
24	13.51	13.51	13.51	13.51	13.51	13.51	13.51

Besides the conventional units providing the required energy, these units are supported up and down reserve capacities. Therefore, Figs. 11.7 and 11.8 indicated the scheduled up and down reserves provided by three generation units, respectively. During peak hours, the high-cost generation unit G2 nearly is provided all of up and down reserve capacity. However, the two other generation units are rendered up and down reserve capability during off-peak hours, which are clarified in these figures.

As stated before, the almost load shedding has taken place in hours 11, 14, and 18, which has caused to curtail demands instead of starting and contributing more expensive generation units in the reserve market. In reality, due to much-low scenario occurrence probability, an independent system operator (ISO) prefers to lessen demands to decrease energy and reserve expenditures. So, the expected load shedding and wind power curtailment are 3.838 MWh and 6.668 MWh, respectively. The related expenditures of providing energy and scheduled reserve capacity are 67833.987$ and 2679.2$, respectively, in which summation of them could report

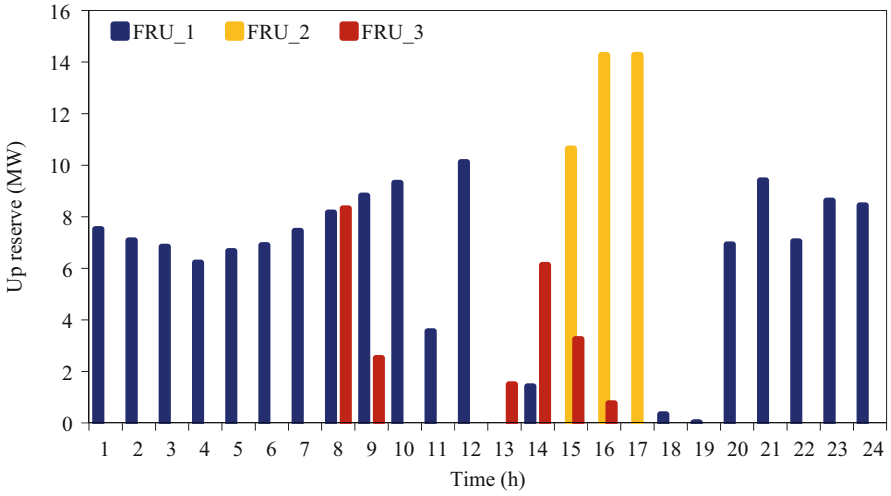

Fig. 11.7 Up scheduled reserve presented by generation units in Case 1

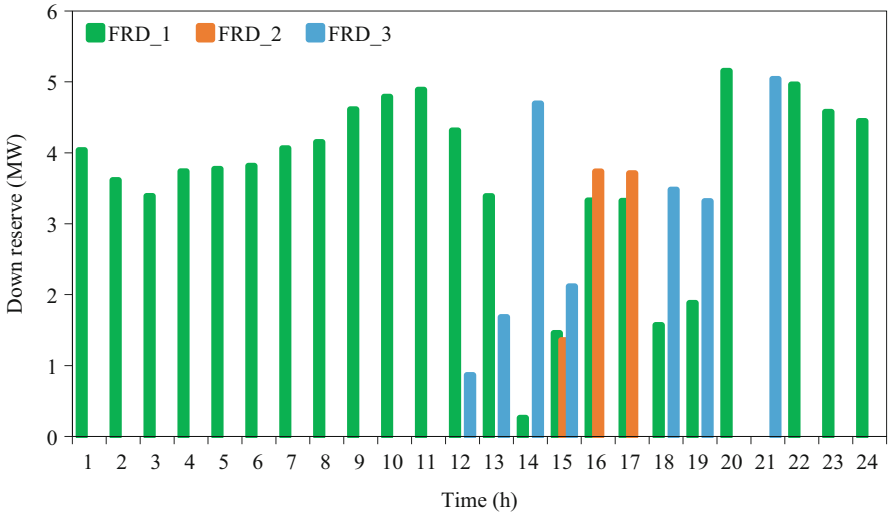

Fig. 11.8 Down scheduled reserve presented by generation units in Case 1

the entire operating cost. Besides, load shedding and wind power curtailment costs are precisely equivalent to 1533.870$ and 333.380$, respectively.

Case 2 In this case, HSS technology is considered and added to the discussed units in Case 1. The scheduled charge and discharge power of HSS is demonstrated in Fig. 11.9. As shown in this figure, during peak periods (i.e., hours 15–17), the discharging mode has happened due to reducing the costs, while the charging mode

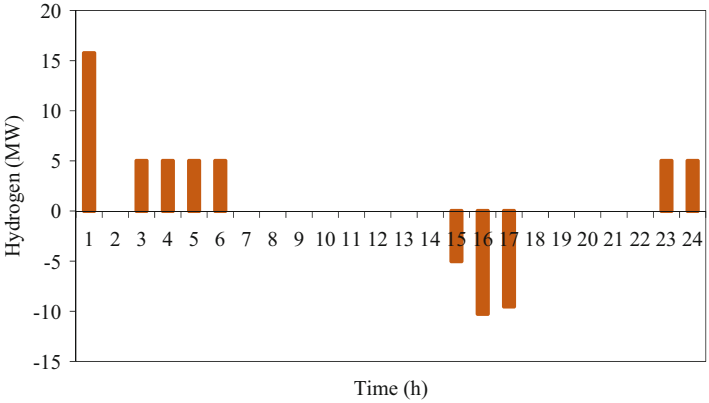

Fig. 11.9 The scheduled charge/discharge power of HSS

takes place during off-peak times (i.e., hours 1–6 and 23–24). Furthermore, the presence of HSS in the power dispatch of conventional units has a significant effect on decreasing power generation of high- and medium-cost units. Thus, according to Fig. 11.10, the generated power of high-cost unit G2 is reduced to zero, and also the generated power of medium-cost unit G3 is diminished compared to Case 1 during peak hours; however, produced power of unit G3 increases a relative little during off-peak hours. It is noteworthy that the power generation of low-cost unit G1 is increased a little minor in some peak and off-peak periods compared to Case 1. To analyze the effects of the participation HSS on the up and down reserve capacities provided by conventional generation units, Figs. 11.11 and 11.12 are presented. In the charging mode of HSS, the scheduled down reserve capacity is presented by this facility. Moreover, in this mode and off-peak times, the scheduled down reserve capacity by conventional units has been reduced to zero compared to Case 1, which is depicted in Fig. 11.11. On another side, almost all of the required up reserve capacity is supplied by the HSS unit, and the scheduled up reserve capacity by high-cost unit G2 is decreased to nearly zero during peak hours, as demonstrated in Fig. 11.12.

As well as committing the HSS facility to investigate the noticeable effects on the scheduling energy and reserve of units and their related costs, LMPs in each hour have been affected by this added unit. Therefore, all LMPs in the presence of the HSS unit are listed in Table 11.4. Similar to Case 1, the maximum value of LMPs has happened in hours 11, 14, and 18 that are highlighted in black, which are directly dependent on the congestion of transmission lines. And also, between these three congested hours, the LMP of bus 4 is the highest one compared to the other buses. In addition, in this case, LMPs of some buses are decreased compared to Case 1, in which Fig. 11.13 shows the Avg.LMPs and the reduction level in comparison with Avg.LMPs of Case 1. As it is evident in Fig. 11.13, Avg.LMPs of Case 2 during peak times, i.e., hours 15–17, approximately are reduced by 40% than Case 1.

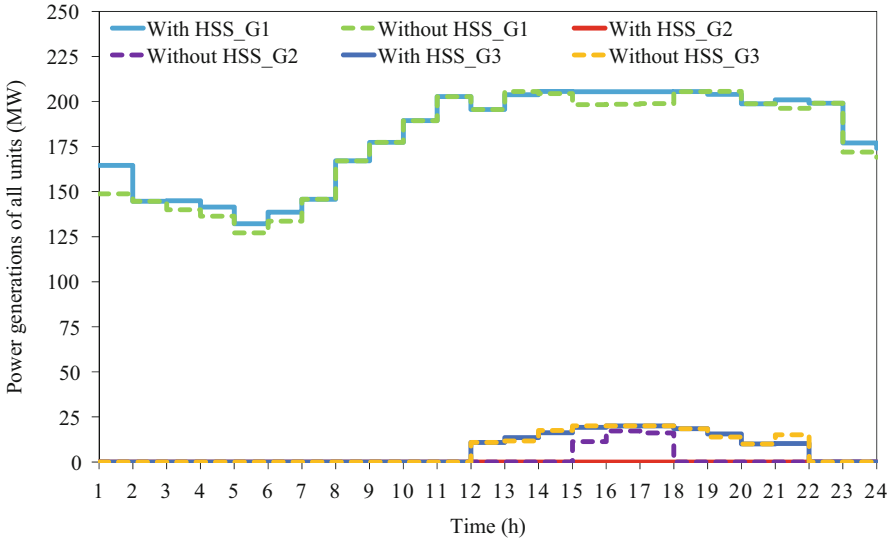

Fig. 11.10 Comparison of hourly power generation in Case 1 and Case 2 for all units

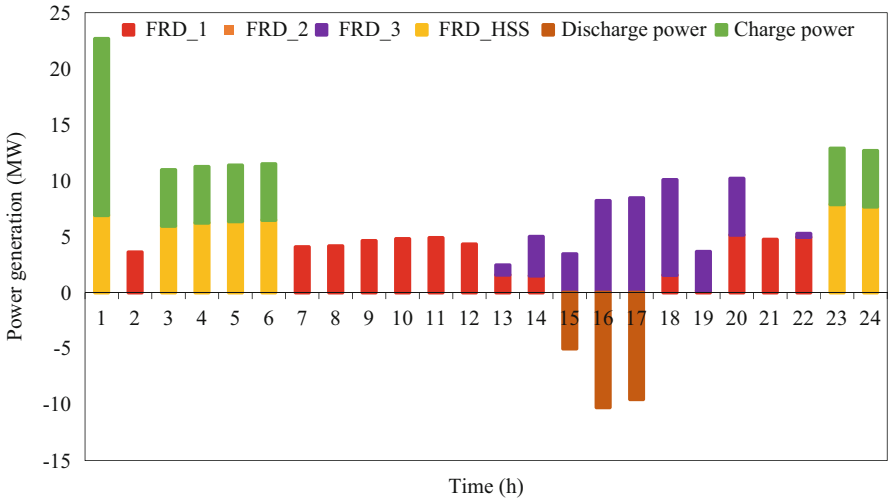

Fig. 11.11 Down scheduled reserve capacity from various units in Case 2

Finally, Table 11.5 is reported and compared the optimal obtained results with Case 1 to investigate the effects of adding HSS unit into the proposed system in terms of total operating cost, including energy and reserve costs, load shedding cost, and wind power curtailment cost. In this case, wind power curtailment has been reduced to 4.357 MWh due to the HSS unit's obligation in providing charge and discharge reserves. Also, the load shedding in this case is equivalent to 3.735 MWh.

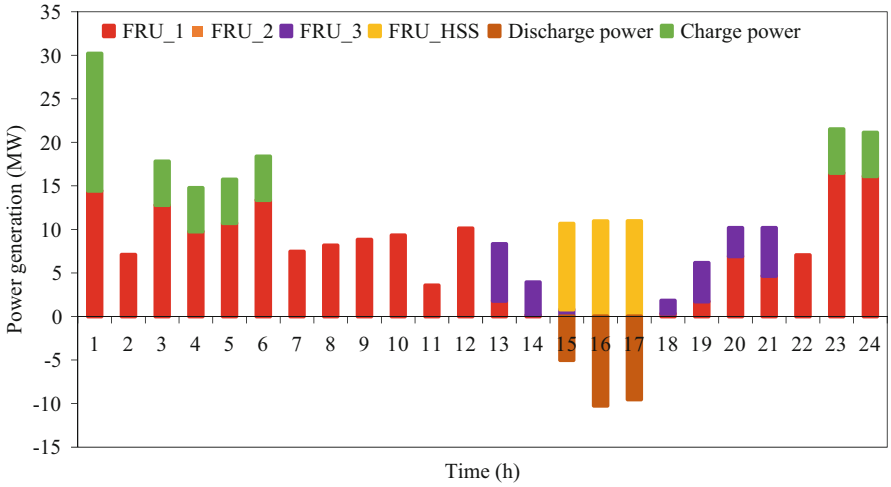

Fig. 11.12 Up scheduled reserve capacity from various units in Case 2

11.5 Conclusions

This chapter proposed a two-stage stochastic network-constrained market-clearing model by considering the integrated fuel cell-based HSS and WES technologies to supply optimal energy and reserve services. In addition, to cover the system uncertainties, i.e., forecasting electrical demand and WES power production errors, the MCS method has been utilized to realize the scheduling problem. In the represented model, both day-ahead and real-time markets are considered a two-stage stochastic programming structure and the determination of energy cost, up and down reserve costs, load shedding, and wind power curtailment. Simulation results indicated that incorporating the HSS facility in the considered six-bus modified electric test system has noticeable effects on the decrement of energy and reserve costs and also in the load shedding and wind power curtailment. So, the percentage reduced levels of total daily scheduling cost, energy cost, and reserve cost are about 3%, 1.4%, and 5.9%, respectively, in the presence of the HSS unit. Besides, electricity prices in peak hours are decreased by 40% by contributing HSS unit. Another significant effect is that it leads to a 35% and 3% reduction in wind power curtailment and electrical load shedding, respectively.

11.6 Status Quo, Challenges, and Outlooks

The status quo of the HSS facility integration into the electric power systems in a coordinated-based approach is about those finite countries such as Canada,

Table 11.4 LMPs of all six buses in Case 2

Time (h)	Bus_1	Bus_2	Bus_3	Bus_4	Bus_5	Bus_6	Avg.LMPs
LMP($/MWh)							
1	13.51	13.51	13.51	13.51	13.51	13.51	13.51
2	13.51	13.51	13.51	13.51	13.51	13.51	13.51
3	13.51	13.51	13.51	13.51	13.51	13.51	13.51
4	13.51	13.51	13.51	13.51	13.51	13.51	13.51
5	13.51	13.51	13.51	13.51	13.51	13.51	13.51
6	13.51	13.51	13.51	13.51	13.51	13.51	13.51
7	13.51	13.51	13.51	13.51	13.51	13.51	13.51
8	13.51	13.51	13.51	13.51	13.51	13.51	13.51
9	13.51	13.51	13.51	13.51	13.51	13.51	13.51
10	13.51	13.51	13.51	13.51	13.51	13.51	13.51
11	**13.51**	**95.34**	**126.3**	**140.8**	**134.2**	**132.5**	**107.2**
12	13.51	15.02	15.61	15.90	15.88	15.83	15.32
13	13.51	26.53	31.40	33.79	32.85	32.85	28.42
14	**13.51**	**95.83**	**127.3**	**141.5**	**135.2**	**132.8**	**107.7**
15	13.51	19.21	21.36	22.46	22.00	21.82	20.06
16	13.51	19.97	22.42	23.59	23.19	22.86	20.92
17	13.51	19.99	22.47	23.59	23.19	22.86	20.92
18	**13.51**	**95.86**	**127.3**	**141.5**	**135.7**	**132.8**	**107.7**
19	13.51	44.23	55.83	61.26	59.15	58.04	48.67
20	13.51	15.02	15.61	15.90	15.88	15.83	15.32
21	13.51	15.69	16.58	16.94	16.79	16.63	16.01
22	13.51	25.75	30.41	32.54	31.64	31.21	27.53
23	13.51	13.51	13.51	13.51	13.51	13.51	13.51
24	13.51	13.51	13.51	13.51	13.51	13.51	13.51

China, France, Germany, Japan, Norway, South Korea, and the USA that are taking part in developing and implementing. With regard to the International Energy Agency's Hydrogen Projects Database, approximately 320 green hydrogen production demonstration projects have been declared globally which have a whole 200 MW electrolyzer capacity. However, some technical challenges have been seen and should be eliminated or reduced significantly to improve as much as possible the full and large-scale integration of HSS technology in various power grids. These challenges and obstacles are efficiency, durability, and investment costs.

The hydrogen's long-term potential and a development roadmap predicted that 18% of global final energy demand could be supplied by hydrogen energy sources until 2050. Decarbonizing transportation is the first realization of HSS that indicates the fuel cell PEVs, high-utilization road vehicles (trucks, buses), ferry boats, and forklifts. The other applications contribute to decarbonizing rail transport, shipping, and aviation in the longer term. In the short term, the injection of hydrogen energy into the natural gas network provides a potential revenue to improve the power-to-

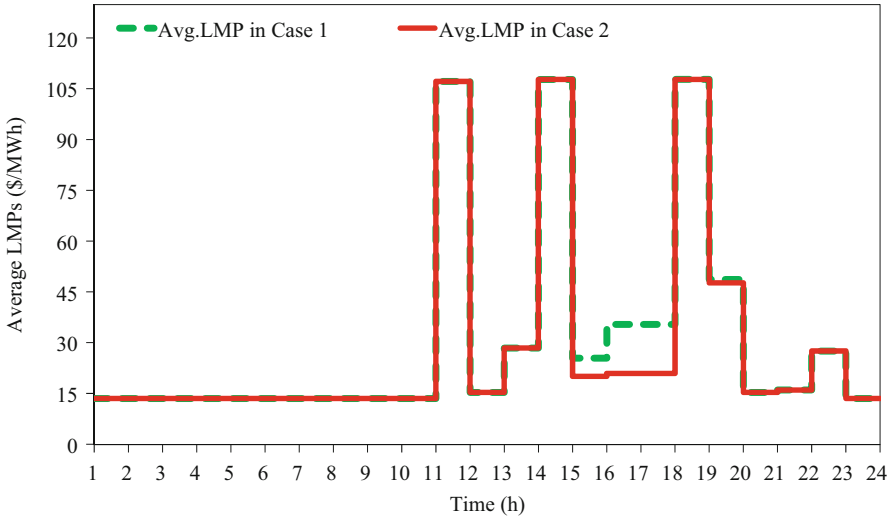

Fig. 11.13 Comparison of Avg.LMPs in Case 1 and Case 2

Table 11.5 Various costs of the proposed system in Case 1 and Case 2

Cases	Total scheduling cost	Energy cost	Reserve cost	Load shedding cost	Wind curtailment cost
Costs($)					
Case 1	73184.201	67833.98	2678.17	1533.870	333.380
Case 2	71463.84	66900.41	2521.09	1503.530	217.859

hydrogen's (P2H) economics however that keeps the promise of storing a major amount of RESs in the long term which decarbonizes demand for natural gas.

Acknowledgements This publication was partially supported by award NPRP12S-0125-190013 from the QNRF-Qatar National Research Fund, a member of The Qatar Foundation. The information and views set out in this publication are those of the authors and do not necessarily reflect the official opinion of the QNRF.

References

1. IRENA (2019) and Abu Dhabi, Future of wind: Deployment, investment, technology, grid integration and socio – Economic aspects (A Global Energy Transformation paper) International Renewable Energy Agency.
2. Heydarian-Forushani, E., Golshan, M. E. H., & Shafie-khah, M. (2016). Flexible interaction of plug-in electric vehicle parking lots for efficient wind integration. *Applied Energy, 179*, 338–349.

3. Wang, S., Yang, H., Pham, Q. B., Khoi, D. N., & Nhi, P. T. T. (2020). An ensemble framework to investigate wind energy sustainability considering climate change impacts. *Sustainability, 12*(3), 876.
4. Ela, E., et al. (2016). Wholesale electricity market design with increasing levels of renewable generation: Incentivizing flexibility in system operations. *The Electricity Journal, 29*(4), 51–60.
5. Alipour, M., Mohammadi-Ivatloo, B., Moradi-Dalvand, M., & Zare, K. (2017). Stochastic scheduling of aggregators of plug-in electric vehicles for participation in energy and ancillary service markets. *Energy, 118*, 1168–1179.
6. Daneshvar, M., Mohammadi-Ivatloo, B., Zare, K., & Asadi, S. (2020). Two-stage stochastic programming model for optimal scheduling of the wind-thermal-hydropower-pumped storage system considering the flexibility assessment. *Energy, 193*.
7. García-Garre, A., Gabaldón, A., Álvarez-Bel, C., Ruiz-Abellón, M. D. C., & Guillamón, A. (2018). Integration of demand response and photovoltaic resources in residential segments. *Sustainability, 10*(9), 3030.
8. Xu, Q., Ding, Y., & Zheng, A. (2017). An optimal dispatch model of wind-integrated power system considering demand response and reliability. *Sustainability, 9*(5), 758.
9. Aliasghari, P., Mohammadi-Ivatloo, B., Alipour, M., Abapour, M., & Zare, K. (2018). Optimal scheduling of plug-in electric vehicles and renewable micro-grid in energy and reserve markets considering demand response program. *Journal of Cleaner Production, 186*, 293–303.
10. Mirzaei, M. A., Sadeghi Yazdankhah, A., & Mohammadi-Ivatloo, B. (2019). Stochastic security-constrained operation of wind and hydrogen energy storage systems integrated with price-based demand response. *International Journal of Hydrogen Energy, 44*(27), 14217–14227.
11. Yu, D., Wang, J., Li, D., Jermsittiparsert, K., & Nojavan, S. (2019). Risk-averse stochastic operation of a power system integrated with hydrogen storage system and wind generation in the presence of demand response program. *International Journal of Hydrogen Energy, 44*(59), 31204–31215.
12. Mansour-Saatloo, A., Mirzaei, M. A., Mohammadi-Ivatloo, B., & Zare, K. (2020). A risk-averse hybrid approach for optimal participation of power-to-hydrogen technology-based multi-energy Microgrid in multi-energy markets. *Sustainable Cities and Society, 63*.
13. Mansour-Saatloo, A., Agabalaye-Rahvar, M., Mirzaei, M. A., Mohammadi-Ivatloo, B., Abapour, M., & Zare, K. (2020). Robust scheduling of hydrogen based smart micro energy hub with integrated demand response. *Journal of Cleaner Production, 267*.
14. Seyyedeh-Barhagh, S., Majidi, M., Nojavan, S., & Zare, K. (2019). Optimal scheduling of hydrogen storage under economic and environmental priorities in the presence of renewable units and demand response. *Sustainable Cities and Society, 46*.
15. Dhabi, A. (2019). *Hydrogen: A renewable energy perspective*. IRENA, International Renewable Energy Agency.
16. *ThyssenKrupp's "green hydrogen and renewable ammonia value chain*. Ammon. Ind. ammoniaindustry.com/thyssenkrupps-green-hydrogen-and-renewable-ammonia-value-chain/."
17. Fernandez-Blanco, R., Arroyo, J. M., & Alguacil, N. (2014). Network-constrained day-ahead auction for consumer payment minimization. *IEEE Transactions on Power Systems, 29*(2), 526–536.
18. Parvania, M., Fotuhi-Firuzabad, M., & Shahidehpour, M. (2014). Comparative hourly scheduling of centralized and distributed storage in day-ahead markets. *IEEE Transactions on Sustainable Energy, 5*(3), 729–737.
19. Agabalaye-Rahvar, M., Mansour-Saatloo, A., Mirzaei, M. A., Mohammadi-Ivatloo, B., Zare, K., & Anvari-Moghaddam, A. (2020). Robust optimal operation strategy for a hybrid energy system based on gas-fired unit, power-to-gas facility and wind power in energy markets. *Energies, 13*(22).
20. Nasri, A., Kazempour, S. J., Conejo, A. J., & Ghandhari, M. (2016). Network-constrained AC unit commitment under uncertainty: A benders' decomposition approach. *IEEE Transactions on Power Systems, 31*(1), 412–422.

21. Tumuluru, V. K., & Tsang, D. H. K. (2018). A two-stage approach for network constrained unit commitment problem with demand response. *IEEE Transactions on Smart Grid, 9*(2), 1175–1183.
22. Kia, M., Nazar, M. S., Sepasian, M. S., Heidari, A., & Siano, P. (2017). Optimal day ahead scheduling of combined heat and power units with electrical and thermal storage considering security constraint of power system. *Energy, 120*, 241–252.
23. Nazari-Heris, M., Mohammadi-Ivatloo, B., & Asadi, S. (2020). Optimal operation of multi-carrier energy networks considering uncertain parameters and thermal energy storage. *Sustainability, 12*(12), 5158.
24. Vahedipour-Dahraie, M., Najafi, H., Anvari-Moghaddam, A., & Guerrero, J. (2017). Study of the effect of time-based rate demand response programs on stochastic day-ahead energy and reserve scheduling in islanded residential Microgrids. *Applied Sciences, 7*(4).
25. Doostizadeh, M., Aminifar, F., Ghasemi, H., & Lesani, H. (2016). Energy and reserve scheduling under wind power uncertainty: An adjustable interval approach. *IEEE Transactions on Smart Grid, 7*(6), 2943–2952.
26. Cobos, N. G., Arroyo, J. M., Alguacil, N., & Wang, J. (2018). Robust energy and reserve scheduling considering bulk energy storage units and wind uncertainty. *IEEE Transactions on Power Systems, 33*(5), 5206–5216.
27. Mirzaei, M. A., Yazdankhah, A. S., Mohammadi-Ivatloo, B., Marzband, M., Shafie-khah, M., & Catalão, J. P. S. (2019). Stochastic network-constrained co-optimization of energy and reserve products in renewable energy integrated power and gas networks with energy storage system. *Journal of Cleaner Production, 223*, 747–758.
28. Jain, I. P., Jain, P., & Jain, A. (2010). Novel hydrogen storage materials: A review of lightweight complex hydrides. *Journal of Alloys and Compounds, 503*(2), 303–339.
29. Meregalli, V., & Parrinello, M. (2001). Review of theoretical calculations of hydrogen storage in carbon-based materials. *Applied Physics A Materials Science & Processing, 72*(2), 143–146.
30. Demirci, U. B. (2017). Ammonia borane, a material with exceptional properties for chemical hydrogen storage. *International Journal of Hydrogen Energy, 42*(15), 9978–10013.
31. Heo, Y.-J., Yeon, S.-H., & Park, S.-J. (2019). Defining contribution of micropore size to hydrogen physisorption behaviors: A new approach based on DFT pore volumes. *Carbon, 143*, 288–293.
32. Maniyali, Y., Almansoori, A., Fowler, M., & Elkamel, A. (2013). Energy hub based on nuclear energy and hydrogen energy storage. *Industrial & Engineering Chemistry Research, 52*(22), 7470–7481.
33. Mansour-Satloo, A., Agabalaye-Rahvar, M., Mirazaei, M. A., Mohammadi-Ivatloo, B., Zare, K., & Anvari-Moghaddam, A. (2021). A hybrid robust-stochastic approach for optimal scheduling of interconnected hydrogen-based energy hubs. *IET Smart Grid, 4*(2), 241–254.
34. Soroudi, A., Aien, M., & Ehsan, M. (2012). A probabilistic modeling of photo voltaic modules and wind power generation impact on distribution networks. *IEEE Systems Journal, 6*(2), 254–259.
35. Mansour-Saatloo, A., Agabalaye-Rahvar, M., Mirzaei, M. A., Mohammadi-Ivatloo, B., & Zare, K. (2021). Chapter 9 – Economic analysis of energy storage systems in multicarrier microgrids. In B. Mohammadi-Ivatloo, A. Mohammadpour Shotorbani, & A. Anvari-Moghaddam (Eds.), *Energy storage in energy markets* (pp. 173–190). Academic Press.
36. Alabdulwahab, A., Abusorrah, A., Zhang, X., & Shahidehpour, M. J. I. S. J. (2015). Stochastic security-constrained scheduling of coordinated electricity and natural gas infrastructures. *IEEE Systems Journal, 11*(3), 1674–1683.
37. Sun, W. L. L., Xu, B., & Chai, T. (2010). *The scheduling of steel-making and continuous casting process using branch and cut method via CPLEX optimization*. In 5th International conference on computer sciences and convergence information technology, pp. 716–721.